Probing Proton Damage in SOI CMOS Technology by Using Lateral Bipolar Action

Ying Li, *Student Member, IEEE*, Guofu Niu, *Senior Member, IEEE*, John D. Cressler, *Fellow, IEEE*, Jagdish Patel, *Member, IEEE*, Mike Liu, *Member, IEEE*, Mohammad M. Mojarradi, *Member, IEEE*, Robert A. Reed, *Member, IEEE*, Paul W. Marshall, *Member, IEEE*, and Benjamin J. Blalock, *Member, IEEE*

***Abstract*—We investigate proton damage in SOI CMOS devices on UNIBOND using a variety of lateral bipolar operational modes. We show that the impact of interface states and oxide charge can be more clearly observed using lateral bipolar action than by using normal FET operational characteristics. We also investigate the radiation-induced interface states at the Si/buried oxide interface and oxide charges in the buried oxide of this SOI CMOS technology using the DCIV method.**

***Index Terms*—Interface states, interface traps, lateral bipolar, proton radiation, SOI.**

I. Introduction

IT is well known that proton radiation produces both displacement and ionization damage in semiconductor devices. In MOSFET characterization, the subthreshold $I_D - V_{GS}$ characteristics are widely used to determine the number of interface traps introduced by irradiation, as well as the resulting radiation-induced fixed oxide trapped charges. The induced change of the $I_D - V_{GS}$ characteristics, however, is often very small, making the identification of radiation-induced charges difficult, primarily because of the thin gate oxide found in modern devices. On the other hand, the gate-controlled base current (I_B) or gate-diode current (I_{GD}) can be used to measure the recombination current due to the interface traps generated at the Si/SiO_2 interface during fabrication, under stress, or after radiation, when an MOSFET is operated as a lateral bipolar transistor [1]–[5] or as a gated diode (body to source/drain) [6]–[8]. Electrical properties of the interface traps, including their energy levels and density, can be derived from the gate bias dependence of the recombination current [9]–[11], an analysis technique which can be dated back to the early 1960s [12], [13].

We propose in this paper a new technique for identifying radiation-induced charge by using the collector current characteristics of a lateral bipolar transistor, and demonstrate its utility by applying it to the analysis of proton radiation damage in SOI CMOS devices on UNIBOND. This technique, together with conventional $I_D - V_{GS}$ measurements and direct-current current-voltage (*DCIV*) measurements [1], provides an effective toolset for radiation damage probing of advanced transistor technologies. We also investigate the radiation-induced interface states and oxide trapped charge for the back-gate transistor in SOI CMOS technologies using the *DCIV* method. The back-gate *DCIV* spectra (I_B versus back-gate V_{GB} curves) clearly shows the radiation-induced changes in interface states at the Si/buried oxide interface, as well as fixed oxide charges trapped in buried oxide during irradiation and, hence, is very useful for diagnostics of irradiated devices.

II. Experiment

The devices were fabricated using Honeywell's 0.35 μm partially depleted SOI technology [14]. The SOI substrate here was formed by UNIBOND. The buried oxide thickness was 400 nm. The silicon film thickness was 225 and 215 nm before and after device processing, respectively. Total dose radiation hardening of the front gates, back gates, and field oxides was accomplished by appropriate steps in the CMOS process flow. The doping in the silicon film is not uniform but averages $3 \times 10^{17}\ \mathrm{cm}^{-3}$. A single n^+ doped polysilicon gate is used. The transistor has a 8 nm thick gate oxide, and a CVD oxide refilled shallow trench. Both nFETs and pFETs have lightly doped drain (LDD) structures to improve hot electron reliability. The body tie is formed by a connection at each end of the gate [16], [17].

The wafers were diced and attached to a ceramic holder and directly exposed to 62.5 MeV protons to equivalent gamma doses as high as 3 Mrad(Si) at the Crocker Nuclear Laboratory Cyclotron located at the University of California at Davis. The dosimetry measurements used a 5-foil secondary emission monitor calibrated against a Faraday cup. Ta scattering foils located several meters upstream of the target establish a beam spatial uniformity of 15% over a 2 cm radius circular area. Beam currents from about 5 pA to 50 nA allow testing with proton fluxes from 10^6 to $10^{12}\ \mathrm{protons/cm^2/s}$. The dosimetry system has been previously described [18], [19] and is accurate to about 10%. At a proton fluence of $1 \times 10^{12}\ \mathrm{p/cm^2}$, the measured equivalent gamma dose was approximately 136 krad(Si).

Manuscript received July 15, 2003; revised September 11, 2003. This work was supported by the JPL CISM program under Contract 1219281, DTRA under the Radiation Tolerant Microelectronics Program, NASA-GSFC under the Electronics Radiation Characterization (ERC) Program, and the Auburn University CSPAE under NASA Contract NCC5-549. The samples were fabricated at the Honeywell Solid State Electronics Center.

Y. Li and G. Niu are with the Alabama Microelectronics Science and Technology Center, Electrical and Computer Engineering Department, Auburn University, Auburn, AL 36849 USA (e-mail: yingli@eng.auburn.edu).

J. D. Cressler is with the School of Electrical and Computer Engineering, Georgia Institute of Technology, Atlanta, GA 30332 USA.

J. Patel and M. M. Mojarradi are with the Jet Propulsion Laboratory, Pasadena, CA 91109 USA.

M. Liu is with the Honeywell Solid State Electronics Center, Plymouth, MN 55441 USA.

R. A. Reed is with the NASA-GSFC, Code 562, Greenbelt, MD 20771 USA.

P. W. Marshall is a consultant to NASA-GSFC, Code 562, Greenbelt, MD 20771 USA.

B. J. Blalock is with the Department of Electrical and Computer Engineering, University of Tennessee, Knoxville, TN 37966 USA.

Digital Object Identifier 10.1109/TNS.2003.822088

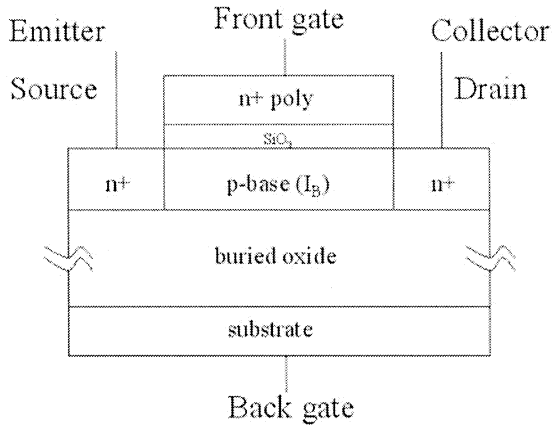

(a)

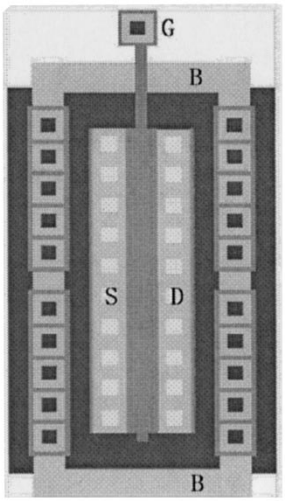

(b)

Fig. 1. (a) Cross-section view of the basic SOI MOSFET structure. (b) Layout of a 10/0.35 SOI nFET with body ties.

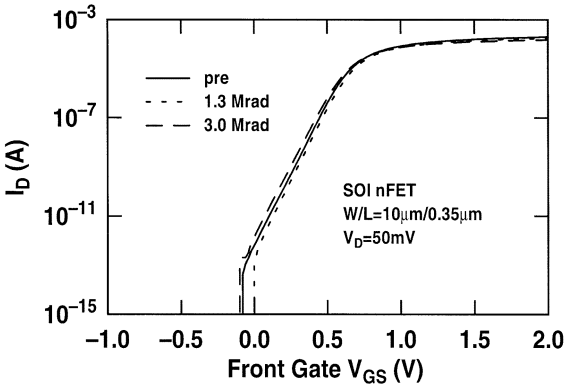

Fig. 2. Front-gate subthreshold characteristics of a 10/0.35 SOI nFET.

An array of SOI nFETs and pFETs with three different lengths ($\mathrm{W/L} = 10\ \mu\mathrm{m}/0.35\ \mu\mathrm{m}$, $10\ \mu\mathrm{m}/0.5\ \mu\mathrm{m}$ and $10\ \mu\mathrm{m}/10\ \mu\mathrm{m}$) were measured before and after radiation. During irradiation, the device terminals were floating, and does not represent the worst case bias conditions.

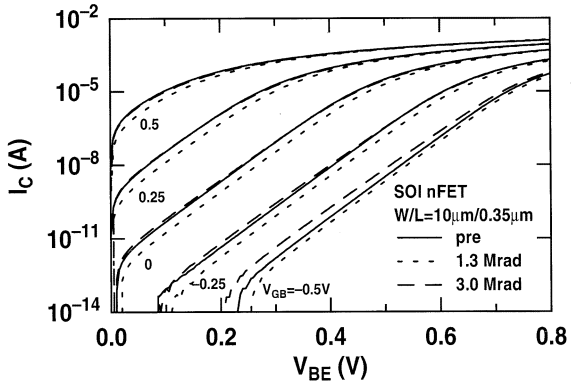

Fig. 3. The collector current versus the base-emitter current for a 10/0.35 SOI nFET at the different gate-base voltages.

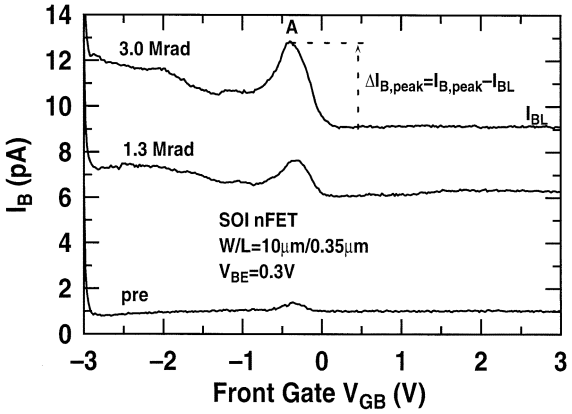

Fig. 4. The gate-controlled I_B curves for a 10/0.35 nFET.

The schematic cross-section of these SOI MOSFETs is shown in Fig. 1(a). The body ties of the device cannot be seen in this two-dimensional view because they are at the two ends of the front-gate, as shown in Fig. 1(b).

III. Measurement Technique

In our measurements, the front-gate controlled I_B (also called the "*DCIV* spectra" [1]) of the n^+ source (emitter)/p^- body (base)/n^+ drain (collector) lateral BJT for the nFET, and p^+ source (emitter)/n^- body (base)/p^+ drain (collector) lateral BJT for the pFET ($V_{SB} = V_{DB} = -V_{BE}$), was used to probe the recombination current from the interface traps which are distributed over the front-gate channel region. We also define a back-gate controlled mode by sweeping the back-gate voltage to obtain the base current I_B. Because the drain/source junctions penetrate the entire silicon film in this technology, under this back-gate controlled mode measurement, the base current can be also used to measure the recombination current from the interface traps generated during irradiation (or even fabrication) in the back-gate channel region (back-gate *DCIV* spectra). The collector current characteristics of this front-gate controlled lateral bipolar transistor are also used to identify the radiation-induced charge.

IV. Results and Discussion

A. Front-Gate Transistor

Consider first an SOI MOSFET exposed to 1.3 Mrad and 3 Mrad radiation levels. The pre- and post-radiation front-gate $I_D - V_{GS}$ characteristics are shown in Fig. 2 for a 10/0.35 ($\mathrm{W/L} = 10\ \mu\mathrm{m}/0.35\ \mu\mathrm{m}$) nFET. A close inspection shows that the threshold voltage first increases with increasing dose, and then decreases with further dose. The threshold voltage is 0.64 V, 0.65 V, and 0.61 V at pre-radiation, after 1.3 and 3 Mrad, respectively. This can be attributed to the combined effects of interface traps (which increases V_{th}) and oxide trapped charge (which decreases V_{th}) [14]. The shift of the subthreshold $I_D - V_{GS}$ characteristics, however, is quite small, because of the thin front gate oxide (8 nm in this case). The subthreshold swing is 86.6 mV/decade before radiation and 89.3 mV/decade after 3 Mrad radiation. Furthermore, it is impossible to make any meaningful identification of the shift in the subthreshold I_D for lower front gate voltages, since I_D is below the measurement resolution limit (10^{-14} A). This is unfortunate, since this shift gives useful information on the interface trap density for traps near the middle of the bandgap.

Recall that the subthreshold drain current can also be viewed as the collector current of the underlying lateral bipolar transistor. The essential difference between this device and a standard BJT is that the base bias is provided through the gate oxide capacitance [15]. We can therefore increase the drain current by simply forward-biasing the source-body junction, which provides a much stronger bipolar action. To better examine the properties of the radiation-induced interface charges as a function of gate voltage, we measured the collector current I_C (or the drain current) as a function of base-emitter voltage V_{BE} (or body-source voltage) using the gate-body voltage (V_{GB}) as a variable. Typical results are shown in Fig. 3 for the same device shown in Fig. 2. The collector is grounded and thus $V_{CB} = 0$ V. The $I_C - V_{BE}$ characteristics are typical of a bipolar transistor except at high V_{GB} and high V_{BE}, when the surface is inverted. The benefits of such a bipolar operation measurement include: 1) the net charge at the interface is more easily identified for each gate voltage and 2) The interface trap information at lower V_{GB} (negative V_{GB} in this case and hence near the middle of the bandgap) can be obtained, due to the higher I_C enabled by the explicit forward V_{BE}.

In Fig. 3, at $V_{GB} = -0.5$ V, one can clearly identify a decrease of I_C at 1.3 Mrad, and a subsequent increase of I_C as the radiation dose increases to 3 Mrad. This observation is consistent with what one would expect by extrapolating the subthreshold $I_D - V_{GS}$ curve to the lower V_{GS} range. However, the identification from Fig. 3 is direct, and much easier in practice. At $V_{GB} = 0$ V, the I_C at 1.3 Mrad is obviously lower than at pre-radiation, and the I_C at 3 Mrad is about the same as at pre-radiation. Therefore, we believe that this new technique using the collector current characteristics of a lateral bipolar transistor can be used to identify radiation-induced charge clearly and probe the radiation damage in these SOI CMOS devices on UNIBOND. While we recognize that the sample size used in this study is small, and thus potentially problematic in resolving the small device parameter changes observed, we point out that very similar behavior in our earlier SOI CMOS investigations were also seen [14], lending support to our present claims.

The front-gate controlled I_B curves with a V_{BE} of 0.3 V are given in Fig. 4 for the same device shown in Fig. 3. The radiation-generated increase of I_B gives a direct measure of the surface recombination velocity S_0 and the density of the interface traps, N_{IT}, because they are proportional to the maximum of the radiation-induced ΔI_B [1]. Here, $\Delta I_B = I_B - I_{BL}$, where I_{BL} is the V_{GB} independent baseline. The baseline current I_{BL} physically comes from electron-hole recombination in the bulk and surface traps located outside the p-channel, and hence are not modulated by the gate voltage V_{GB} [20] when the channel is in accumulation. However, in Fig. 4, the increase of base current with radiation dose in the accumulation region can be clearly observed and is attributed to majority carrier tunneling at the p/n junction perimeter under the gate oxide [20]. With increasing radiation dose, this majority carrier tunneling process increases because the radiation-induced displacement damage increases the number of defects at the corner of gate and drain (source) regions. The pre-radiation I_B peak can only be associated with the interface traps introduced during the fabrication of the device itself. A similar increase of I_B after radiation can also be observed for a 10/0.35 pFET.

The density of the interface traps N_{it} introduced by proton irradiation for the 10/0.35 nFET in Fig. 4, can be determined by this excess recombination current ($\Delta I_{\mathrm{B,peak}} = (I_{\mathrm{B,peak}} - I_{BL})$) for a single-level trap from (3) [1]

$$\Delta I_{\mathrm{B,peak}} = \left(\frac{qA_g n_i S_0}{2}\right) \exp\left(\frac{qV_{BE}}{2kT}\right) \tag{1}$$

$$S_0 = \left(\frac{\pi}{2}\right) \sigma_0 \Theta_{\mathrm{th}} N_{\mathrm{it}}. \tag{2}$$

Therefore

$$N_{\mathrm{it}} = \frac{\Delta I_{\mathrm{B,peak}}}{\left(\frac{\pi}{4}\right) qA_g n_i \sigma_0 \Theta_{\mathrm{th}} \exp\left(\frac{qV_{BE}}{2kT}\right)}. \tag{3}$$

In the above equation, q is electron charge, $A_g = W \times L$ is the gate area, $\sigma_0 = 3 \times 10^{-15}\ \mathrm{cm}^2$ is the trap capture cross-section [20], Θ_{th} is the thermal velocity, n_i is the intrinsic carrier concentration. The calculated N_{it} is $0.86 \times 10^9\ \mathrm{cm}^{-2}$, $3.44 \times 10^9\ \mathrm{cm}^{-2}$ and $8.49 \times 10^9\ \mathrm{cm}^{-2}$ for the 10/0.35 nFET before radiation, after 1.3 Mrad radiation and 3 Mrad radiation, respectively.

Fig. 5 shows the channel length normalized $\Delta I_{B,peak}$ versus dose for 10/0.35, 10/0.5, 10/10 nFETs having the same channel width, but different channel lengths. It can be clearly seen that the value of the $\Delta I_{\mathrm{B,peak}}$ is channel-length dependent, because the radiation-induced interface traps are distributed along the front gate channel. We can also see that the $\Delta I_{\mathrm{B,peak}}$ increases with radiation dose for each device and has not reached a saturation value up to 3 Mrad total dose, which means the N_{it} is not saturated at the front Si/oxide interface up to 3 Mrad. It is clearly shown that the shorter devices experience a more rapid increase of $\Delta I_{\mathrm{B,peak}}$ in Fig. 5 although $\Delta I_{\mathrm{B,peak}}$ is already normalized by channel length. This can be explained by the nonuniform recombination rate at the Si/oxide interface which is determined by the electric field along the p-channel. The shorter the devices are, the stronger their electric fields along the p-channel are and, thus, the more sensitive they are to interface traps. Therefore, the

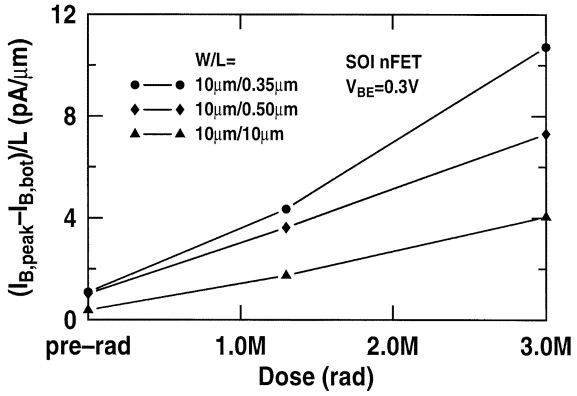

Fig. 5. Channel length normalized ΔI_B peak versus dose for a 10/0.35, 10/0.50, and 10/10 nFETs.

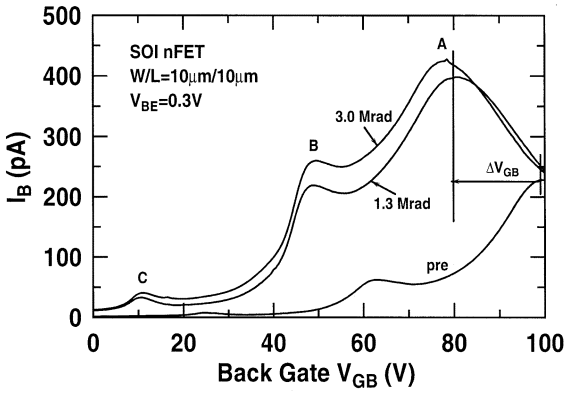

Fig. 6. Back-gate controlled I_B curves for a 10/10 nFET at $V_{BE} = 0.3$ V.

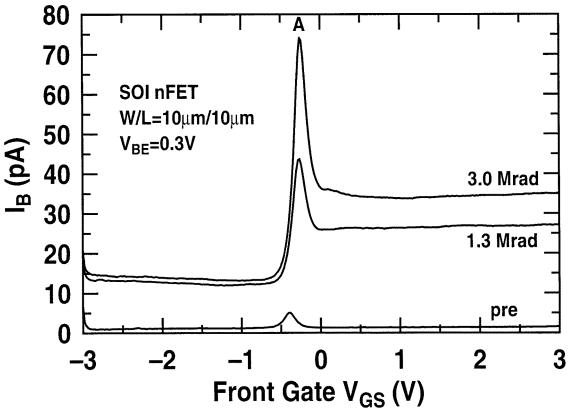

Fig. 7. The front-gate *DCIV* spectra for a 10/10 nFET.

shorter devices experience a more rapid increase of $\Delta I_{\mathrm{B,peak}}$ than in the longer devices. Actually, when the channel length is small, the whole area underneath the gate cannot be treated as a uniform surface for recombination, because of the lateral fields. It is plausible that the radiation induced N_{it} could be different laterally.

B. Back-Gate Transistor

The back-gate controlled I_B is measured when the front-gate channel is accumulated (front-gate $V_{GB} = -1\ V$ for the nFET and front-gate $V_{GB} = 1\ V$ for the pFET) to minimize recombination at the Si/front-gate oxide interface. The measured I_B is then primarily due to recombination at the Si/buried oxide interface or in the silicon film body. The back-gate controlled I_B for a 10/10 nFET is shown in Fig. 6 at $V_{BE} = 0.3$ V. Three peaks (peak A, peak B, and peak C) can be clearly observed for both pre- and post-radiation. Note that I_B increases after radiation, which is attributed to the increase of the number of recombination centers due to radiation damage.

The increases of I_B in Fig. 6 are mainly caused by an increase of (back channel) surface recombination instead of bulk recombination, as explained below. First, the back gate voltage dependence of I_B is too strong to be explained by bulk recombination. I_B varies from 10 pA at 0 V V_{GB} to 400 pA at its peak. Second, if bulk recombination dominates, the I_B would *decrease monotonically* with increasing back gate voltage, because of increasing depletion layer thickness and hence decreasing neutral base volume available for bulk recombination. This is clearly not the case in Fig. 6. The multiple peak characteristics of I_B as a function of back gate V_{GB} can only be explained using multiple energy level recombination centers located at the back channel surface. For further confirmation, we compare the I_B values from back gate voltage sweep to that from front gate voltage sweep. Fig. 7 shows the front-gate *DCIV* spectra with the same V_{BE} of 0.3 V for the same 10/10 nFET. It can be clearly seen that the maximum of the base line of I_B, which indicates maximum bulk recombination that occurs with an accumulated front gate surface, is about 35 pA. However, the I_B in Fig. 6 is hundreds of pA. This further supports that the radiation-induced increases of I_B in Fig. 6 are from back gate surface recombination instead of bulk recombination.

In the MOSFET back-gate $I_D - V_{GS}$ curves, a nearly parallel shift occurs after radiation, as shown in Fig. 8. Therefore, the dominant charge induced by radiation is oxide trapped charge. Surprisingly, no observable degradation of the MOSFET subthreshold slope can be identified, despite the strong increase of back surface recombination. This indicates that the amount of charges at the interface traps, which is modulated by the gate voltage, is insignificant. A constant slope change is often a result of traps with uniform energy distribution, whose effect on recombination current cannot be easily determined as for single energy level traps. Previously, on electrically stressed MOSFET, a strong degradation of the subthreshold slope and a strong increase of the *DCIV* recombination current were both observed [1]. This, however, is not true in our case for radiation induced damage at the back gate surface. It is conceivable that these radiation-induced interface traps at the back gate Si/SiO_2 interface act as effective recombination centers, but trap only a small amount of carriers.

Unlike the MOSFET subthreshold $I_D - V_{GS}$ curves, the post-irradiation *DCIV* spectra is not a simple shift of the pre-irradiation *DCIV* spectra, as shown in Fig. 6. However, the shifts of the voltage position of the peaks (ΔV_{GB}) is considerably different from the shifts of the back gate $I_D - V_{GS}$ curves. At 1.3 Mrad, the shifts are 19.5 V for peak A, and 14 V for peaks B and C in *DCIV* spectra. The shift of the subthreshold $I_D - V_{GS}$ curve, however, is 16.8 V at 1.3 Mrad. Given the fact that the shift of the $I_D - V_{GS}$ curve is nearly independent of V_{GS}, we conclude

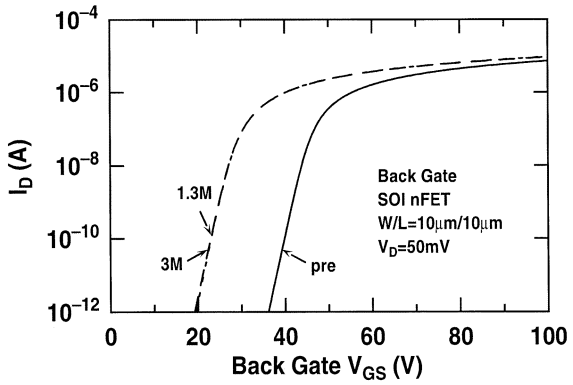

Fig. 8. Back-gate subthreshold characteristics of a 10/10 nFET before and after radiation.

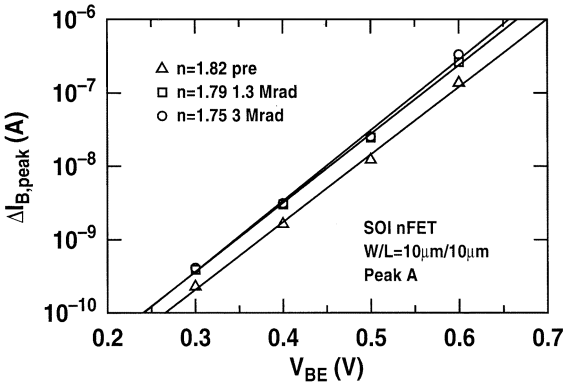

Fig. 9. Variation of $\Delta I_{\mathrm{B,peak}}$ with the forward bias V_{BE} from pre and after two radiation doses. The lines are exponentially fit to the experiment data.

that the energy level distribution of interface traps differs between pre- and post-irradiation. Without a change in the energy level distribution, the change of the *DCIV* spectra would be similar to the change of the $I_D - V_{GS}$, except for an increase in the magnitude of I_B.

A logical question is whether the three peaks observed simply indicate that there are three dominant discrete trap energy levels. To answer this question, we plot $\Delta I_{\mathrm{B,peak}}$ versus V_{BE} on semilog scales for each peak. The result for peak A is shown in Fig. 9. Theory for a discrete energy level interface trap predicts that $\Delta I_{\mathrm{B,peak}} \propto \exp(qV_{BE}/nkT)$, with $n = 1$ when $V_{BE} \ll V_{BE-ET}$, $n = 2$ when $V_{BE} \gg V_{BE-ET}$, and the transition from $n = 1$ to $n = 2$ occurs within 100 mV. Here V_{BE-ET} is determined by the trap energy level as $2(E_T - E_I)/q + [\ln(c_{ns}/c_{ps} - 1.4]kT/q$, with E_T being the trap energy level, E_I being the intrinsic Fermi-level, and C_{ns} and C_{ps} being the electron and hole capture rate coefficients at this trap energy level [20]. The measured data, however, do not show this behavior for peak A, either at pre-radiation or post-radiation. Instead, the data can be fit using a single n factor *over a wide range of* V_{BE}. In this case, $n = 1.82$, 1.79, 1.75 for pre-radiation, at 1.3 Mrad and 3 Mrad doses, respectively. This observed dependence strongly suggests that the distribution of the interface states (both pre- and post-radiation) is relatively flat, despite the three noticeable peaks on the *DCIV* spectra. The shape of the distribution, as discussed above, is changed considerably after irradiation, because of different shifts for the different peaks. We also have determined that the n factor is 1.6 for peak B and 2.0 for peak C at pre-radiation, 1.3 Mrad, and 3 Mrad doses.

Different back-gate controlled I_B curves can be observed in Fig. 10 for a 10/10 pFET, both before and after irradiation. There are only two observable peaks (noted as peak A and peak B) and peak A is much sharper than any peaks observed in the back-gate *DCIV* spectra of the nFETs as shown in Fig. 6. This suggests a more concentrated interface state distribution (in the bandgap) than for the nFET. At 1.3 Mrad, the $I_D - V_{GS}$ shift is -10.3 V, as shown in Fig. 11. The shifts in peak A and B, however, are -15.5 and -10.0 V. This clearly indicates that the energy distribution of the interface traps has changed after irradiation, for reasons similar to that in the nFET case. It is also clearly shown that $I_{\mathrm{B,peak}}$ of peak B equals to that of peak A

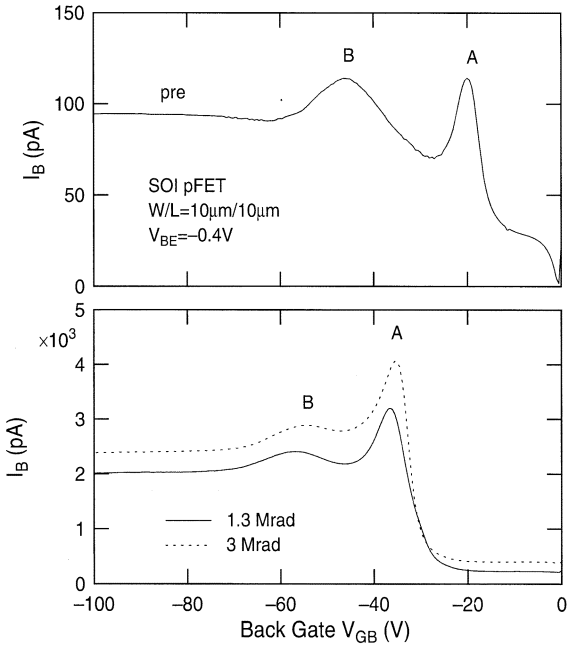

Fig. 10. Back-gate *DCIV* spectra for a 10/10 pFET: 1) pre-radiation; 2) after 1.3 Mrad; and 3) after 3 Mrad.

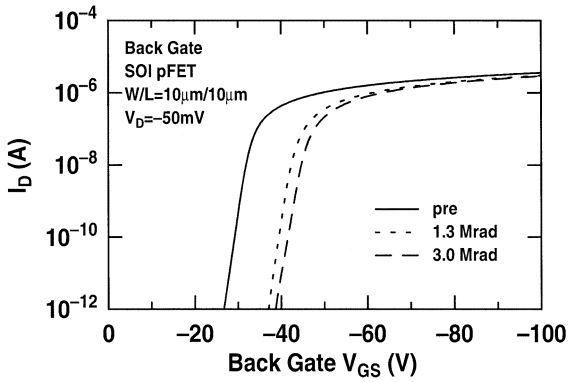

Fig. 11. Back-gate subthreshold characteristics of a 10/10 pFET before and after radiation.

before radiation. However, with increasing radiation dose, the $I_{\mathrm{B,peak}}$ of peak A increases quickly and exceeds that of peak B at 1.3 Mrad radiation. This suggests that radiation-induced

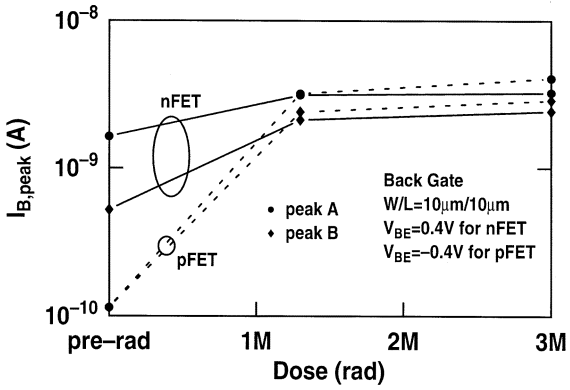

Fig. 12. Back-gate controlled I_B peak versus dose for a 10/10 nFET and a 10/10 pFET.

interface traps are concentrated at the same energy level as that for peak A. Similar I_B versus back-gate V_{GB} characteristics can also be observed for the 10/0.35 pFET. The n factor of $I_{\mathrm{B,peak}}$ for this 10/10 pFET can also be extracted over a wide range of V_{BE} (from $V_{BE} = 0.2$ V to 0.6 V). In this case, for peak A, $\mathrm{n} = 1.42, 1.68, 1.66$ for pre-radiation, at 1.3 Mrad and 3 Mrad doses. For peak B, $\mathrm{n} = 1.30, 1.61, 1.58$ for pre-radiation, at 1.3 and 3 Mrad doses. Therefore, although the radiation-induced interface trap distribution for the pFET is more concentrated than for the nFET, these are not two dominant discrete trap energy levels for the pFET.

Even though the nFETs and pFETs share the same back-gate oxide, they observe a different back-gate radiation response, as can be seen in Fig. 12 for the 10/10 nFET and pFET. It is clearly seen that the recombination current of the pFET back-gate channel is much smaller than that in nFET back-gate channel for pre-irradiation. Below 1.3 Mrad radiation, the I_B peak for the pFET increases more quickly than for the nFET, while above 1.3 Mrad, the recombination current of the pFET is almost as same as that of the nFET. For the nFET, on the other hand, the recombination current saturates after 1.3 Mrad. Note, however, that the recombination current of the pFET still increases, although at a much slower rate than below 1.3 Mrad.

V. Summary

We have investigated radiation damage in SOI CMOS on UNIBOND devices using a new technique which identifies radiation-induced charge using the collector current in bipolar operational mode, and have applied the technique to investigating proton damage in these devices. This technique, together with conventional $I_D - V_{GS}$ measurements and *DCIV* measurements, provides an effective toolset for radiation damage probing of modern SOI technologies. Using *DCIV*, the energy distribution of radiation-induced interface states is investigated for the back-gate transistor in this SOI CMOS technology. We find that the energy distribution of the interface states is significantly changed by proton irradiation. Different back-gate radiation behavior between nFETs and pFETs are clearly observed in the back-gate *DCIV* spectra, suggesting a different damage mechanism between the two devices. Finally, given the small magnitude of the parameter changes we are analyzing, and the small device sample size used in this study, we conclude that our new technique, while promising, will require additional experiments to ensure full validation, and that work is at present underway.

Acknowledgment

The devices were fabricated at Honeywell. The authors would like to thank L. Cohn, K. LaBel, and H. Brandhorst for their support of this work.

References

[1] A. Neugroschel, C.-T. Sah, K. M.K. Michael Han, M. S. Carroll, T. Nishida, J. T. Kavalieros, and Y. Lu, "Direct-current measurements of oxide and interface traps on oxidized silicon," *IEEE Trans. Electron Devices*, vol. 42, pp. 1657–1661, Sept. 1995.

[2] C. T. Sah, A. Neugroschel, K. M.K. Michael Han, and J. T. Kavalieros, "Profiling interface traps in MOS transistors by the DC current-voltage method," *IEEE Electron Device Lett.*, vol. 17, pp. 72–74, Feb. 1996.

[3] J. T. Kavalieros and C. T. Sah, "Separation of interface and nonuniform oxide traps by the DC current-voltage method," *IEEE Trans. Electron Devices*, vol. 43, pp. 137–141, Jan. 1996.

[4] B. B. Jie, M. F. Li, C. L. Lou, W. K. Chim, D. S. H. Chan, and K. F. Lo, "Investigation of interface traps in LDD pMOSTs by the DCIV method," *IEEE Electron Device Lett.*, vol. 18, pp. 583–585, Dec. 1997.

[5] A. Melik-Martirosian and T. P. Ma, "Lateral profiling of interface traps and oxide charge in MOSFET devices: charge pumping versus DCIV," *IEEE Trans. Electron Devices*, vol. 48, pp. 2303–2309, Oct. 2001.

[6] P. Speckbacher, J. Berger, A. Asenov, F. Koch, and W. Weber, "The 'gated-diode' configuration in MOSFETs, a sensitive tool to characterizing hot-carrier degradation," *IEEE Trans. Electron Devices*, vol. 42, pp. 1287–1296, July 1995.

[7] X. Zhao and D. E. Ioannou, "'Gated-diode' in SOI MOSFETs: a sensitive tool for characterizing the buried Si/SiO_2 interface," *IEEE Trans. Electron Devices*, vol. 48, pp. 685–687, Apr. 2001.

[8] R. K. Lawrence, D. E. Ioannou, W. C. Jenkins, and S. T. Liu, "Gated-diode characterization of the back-channel interface on irradiated SOI wafers," *IEEE Trans. Nucl. Sci.*, vol. 48, pp. 2140–2145, Dec. 2001.

[9] G. Niu, G. Banerjee, J. D. Cressler, J. M. Roldan, S. D. Clark, and D. C. Ahlgren, "Electrical probing of surface and bulk traps in proton-irradiated gate-assisted lateral PNP transistors," *IEEE Trans. Nucl. Sci.*, vol. 45, pp. 2361–2365, Dec. 1998.

[10] M.-S. Park and C. R. Wie, "Study of radiation effects in γ-ray irradiated power VDMOSFET by DCIV technique," *IEEE Trans. Nucl. Sci.*, vol. 48, pp. 2285–2293, Dec. 2001.

[11] D. R. Ball, R. D. Schrimpf, and H. J. Barnaby, "Separation of ionization and displacement damage using gate-controlled lateral PNP bipolar transistors," *IEEE Trans. Nucl. Sci.*, vol. 49, pp. 3185–3190, Dec. 2002.

[12] C. T. Sah, "A new semiconductor tetrode—the surface-potential controlled transistor," in *Proc. IRE*, vol. 49, Nov. 1961, pp. 1623–1634.

[13] A. S. Grove and D. J. Fitzelard, "Surface effects on p-n junctions: characteristics of surface space-charge regions under nonequilibrium conditions," *Solid-State Electron.*, vol. 9, pp. 783–806, 1966.

[14] Y. Li, G. Niu, J. D. Cressler, J. Patel, P. W. Marshall, H. S. Kim, S. T. Liu, R. A. Reed, and M. J. Palmer, "Proton radiation effects in 0.35 μm partially-depleted SOI MOSFETs fabrication on UNIBOND," *IEEE Trans. Nucl. Sci.*, vol. 49, pp. 2930–2936, Dec. 2002.

[15] Y. Tsividis, *Operation and Modeling of the MOS Transistor*, 2nd ed. New York: McGraw-Hill, 1999.

[16] S. T. Liu, W. C. Jenkins, and H. L. Hughes, "Total dose radiation hard 0.35 μm SOI CMOS technology," *IEEE Trans. Nucl. Sci.*, vol. 45, pp. 2442–2449, Dec. 1998.

[17] S. T. Liu, S. Balster, S. Sinha, and W. C. Jenkins, "Worst case total dose radiation response of 0.35 μm SOI MOSFETs," *IEEE Trans. Nucl. Sci.*, vol. 46, pp. 1817–1823, Dec. 1999.

[18] K. M. Murray, W. J. Stapor, and C. Castenada, "Calibrated charge particle measurement system with precision dosimetric measurement and control," *Nucl. Instrum. Methods*, vol. B56/57, p. 616, 1991.

[19] P. W. Marshall, C. J. Dale, M. A. Carts, and K. A. Label, "Particle-induced bit errors in high performance fiber optic data lines for satellite data management," *IEEE Trans. Nucl. Sci.*, vol. 41, pp. 1958–1965, Dec. 1994.

[20] J. Cai and C. T. Sah, "Monitoring interface traps by DCIV method," *IEEE Electron Device Lett.*, vol. 20, pp. 60–63, Jan. 1999.